

# HYPERBOLICITY OF AUGMENTED LINKS IN THE THICKENED TORUS

ALICE KWON AND YING HONG THAM

ABSTRACT. For a hyperbolic link  $K$  in the thickened torus, We show there is a decomposition of the complement of a link  $L$ , obtained from augmenting  $K$ , into torihedra. We further decompose the torihedra into angled pyramids and finally angled tetrahedra. These fit into an angled structure on a triangulation of the link complement, and thus by [6], this shows that  $L$  is hyperbolic.

## 1. INTRODUCTION

Given a twist reduced diagram of a link  $K$ , *augmenting* is a process in which an unknotted circle component (augmentation) is added to one or more twist regions (a single crossing or a maximal string of bigons) of  $K$ . The added circle component allows us to remove full twists at the twist region of  $K$ . If the twist region has an odd number of crossings then all but one crossing is removed, whereas if the twist region has an even number of crossings then all are removed. We can remove full twists by a standard argument using a Dehn twist on the complement of the crossing circle. The newly obtained link is called an *augmented link* and the newly obtained diagram is called an *augmented link diagram*. See Figure 2.

Adams showed in [2] that given a hyperbolic alternating link  $K$  in  $S^3$  the link  $L$  obtained by augmenting  $K$  is hyperbolic. In this paper we investigate if this statement holds for links in the thickened torus i.e. if  $L$  is a link obtained from augmenting a hyperbolic alternating link  $K$  in the thickened torus. We define augmenting similarly for links in the thickened torus with their associated link diagram on  $\mathbb{T}^2 \times \{0\}$ .

Menasco [9] showed there are decompositions of the complements of alternating links in  $S^3$  into two topological polyhedra, a top polyhedron and a bottom polyhedron. For alternating links  $K$  in the thickened torus, Champanerkar, Kofman and Purcell [4] showed that there is a decomposition of the complement of  $K$  into objects called torihedra, which we think of as counterparts to Menasco's decomposition of links in  $S^3$  into polyhedra, for links in the thickened torus. Just like Menasco's decomposition, one obtains a top and a bottom torihedron.

In Section 2 we show that for augmented links in the thickened torus one can also obtain a decomposition of the complement into a top and bottom torihedron. In Section 3, we prove that many augmented alternating links in the thickened torus are hyperbolic.

We point out that [7], the first author proved that *fully* augmented links in the thickened torus are hyperbolic, so this paper can be seen as a generalization of that work.

While revising this paper, we learned that [1] proves a generalization of our work here, showing hyperbolicity of generalized augmented links in an arbitrary thickened surface. We note that our approach, based on angle structures, is different from theirs, which is based on topological arguments.

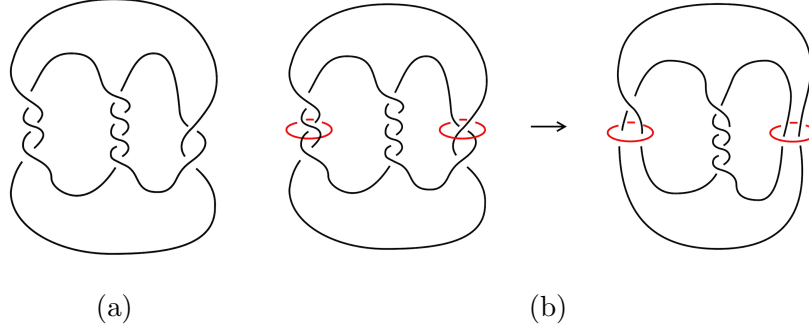


FIGURE 1. The left shows a pretzel knot before augmentation and the right shows after augmentation

## 2. AUGMENTED LINKS

Champanerkar, Kofman and Purcell have studied alternating links in the thickened torus [4]. They define a link in the thickened torus as a quotient of a biperiodic alternating link as follows,

**Definition 2.1.** A *biperiodic alternating link*  $\mathcal{L}$  is an infinite link which has a projection onto  $\mathbb{R}^2$  which is invariant under an action of a two dimensional lattice  $\Lambda$  by translations, such that  $L = \mathcal{L}/\Lambda$  is an alternating link in  $\mathbb{T}^2 \times I$ , where  $I = (-1, 1)$ , with the projection on  $\mathbb{T}^2 \times \{0\}$ .

**Remark 2.2.** Since  $\mathbb{T}^2 \times I \cong S^3 - H$ , where  $H$  is a Hopf link. The complement  $\mathbb{T}^2 \times I - L = S^3 - (L \cup H)$ .

Champanerkar, Kofman and Purcell [4] extended the definition of prime links in  $S^3$  for links in  $\mathbb{T}^2 \times I$  called weakly prime.

**Definition 2.3.** A diagram of a link  $L$  is *weakly prime* if whenever a disk is embedded in the diagram surface meets the diagram transversely in exactly two edges, then the disk contains a simple edge of the diagram and no crossings.

**Definition 2.4.** A *twist region* in a link diagram of  $L = \mathcal{L}/\Lambda$  in  $\mathbb{T}^2 \times I$ , is the quotient of a twist region in the biperiodic link  $\mathcal{L}$ . A biperiodic link  $\mathcal{L}$  is called *twist-reduced* if for any simple closed curve on the plane that intersects the diagram of  $\mathcal{L}$  transversely in four points, with two points adjacent to one crossing and the other two points adjacent to another crossing, the simple closed curve bounds a subdiagram consisting of a (possibly empty) collection of bigons strung end to end between these crossings. We say the diagram of  $L$  is *twist-reduced* if it is the quotient of a twist-reduced biperiodic link diagram.

Now we can define augmentation for a link in  $\mathbb{T}^2 \times I$  the same way we define augmentation for links in  $S^3$ . For a link in  $\mathbb{T}^2 \times I$ , the crossing circles are added to the diagram projected onto  $\mathbb{T}^2 \times \{0\}$ . Let  $D(L)$  be a twist reduced diagram of a link  $L$  in  $\mathbb{T}^2 \times I$ , we define *augmenting* as a process in which an unknotted circle component is added to one or more twist regions of  $D(L)$ . See Figure 2

**Remark 2.5.** If  $L$  is augmented at *every* crossing/twist site we say  $L$  is *fully* augmented.



FIGURE 2. A: The top right has an odd number of twists while the bottom left has an even number of twists. B: The picture of the link on the right after augmentation twist regions circled in red. C: The link with full twists removed.

**2.1. Torihedral Decomposition of Augmented Alternating Links in Thickened Torus.** We present a method of decomposing an augmented link (not necessarily fully augmented) in the thickened torus into objects called “torihedra” as defined below. Decomposing alternating links in the thickened torus into torihedra were first described in [4] then later used for fully augmented links in the thickened torus in [7]. The idea is to combine methods of Menasco [9] and the use of crossing edges between each crossing of our link and Lackenby’s “cut-slice-flatten” method [8] on the augmentation sites.

**Definition 2.6.** [4] A *torihedron*  $\mathcal{T}$  is a cone on the torus, i.e.  $\mathbb{T}^2 \times [0, 1]/(\mathbb{T}^2 \times \{1\})$ , with a cellular graph  $G = G(\mathcal{T})$  on  $\mathbb{T}^2 \times \{0\}$ . The *ideal torihedron*  $\mathcal{T}^\circ$  is  $\mathcal{T}$  with the vertices of  $G$  and the vertex  $\mathbb{T}^2 \times \{1\}$  removed. Hence, an ideal torihedron is homeomorphic to  $\mathbb{T}^2 \times [0, 1]$  with a finite set of points (ideal vertices) removed from  $\mathbb{T}^2 \times \{0\}$ . We refer to the vertex  $\mathbb{T}^2 \times \{1\}$  as the cone point.

For visualization purposes, we typically draw the graph  $G(\mathcal{T})$  of a torihedron from the perspective of the cone point  $\mathbb{T}^2 \times \{1\}$ .

If the faces of  $G(\mathcal{T})$  are disks, then  $\mathcal{T}$  can be decomposed into a union of pyramids, obtained by coning each face to the cone point of  $\mathcal{T}$ . This also gives a decomposition of the corresponding ideal torihedron  $\mathcal{T}^\circ$  into ideal pyramids. We call these the *pyramidal decompositions* of  $\mathcal{T}$  and  $\mathcal{T}^\circ$ .

**Proposition 2.7.** *Let  $L$  be an augmented link in  $\mathbb{T}^2 \times I$ . There is a decomposition of the complement,  $(\mathbb{T}^2 \times I) - L$  into two ideal torihedra.*

*Proof.* We will begin by assuming that there are no half twists. Arrange the link diagram of  $L$  in the following way: first place the added circle components perpendicular to the projection plane,  $\mathbb{T}^2 \times \{0\}$  leaving the remaining part of the link parallel to the projection plane. We now place a crossing edge on each crossing of the link so that for each crossing edge, one end of the edge lies on a bottom strand while the other end lies on a top strand as in Figure 3 left.

We view the link from the point at infinity from the top. We will push the top strand to the bottom strand, splitting the crossing edge into two identical edges as in Figure 3 right. We push the link components to infinity and stretch the crossing edge so that we have flattened the link onto  $\mathbb{T}^2 \times \{0\}$  except for the crossing circles which will remain perpendicular to the projection plane.

Now place a disk on each crossing circle, so that the disk is bounded by the crossing circle. We can then cut  $\mathbb{T}^2 \times I$  along  $\mathbb{T}^2 \times \{0\}$  and focus on the top half,  $\mathbb{T}^2 \times [0, 1]$ . We will follow

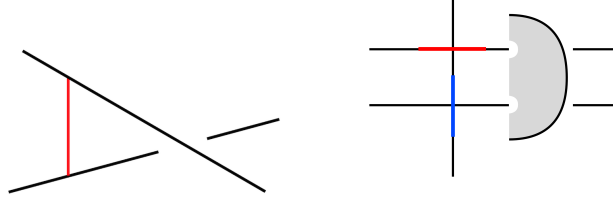


FIGURE 3. Left: The black strands are part of the link and the red strand is the crossing edge. Right: The blue and red edges represent the split crossing edges and the shaded half disk is bounded by the crossing circle

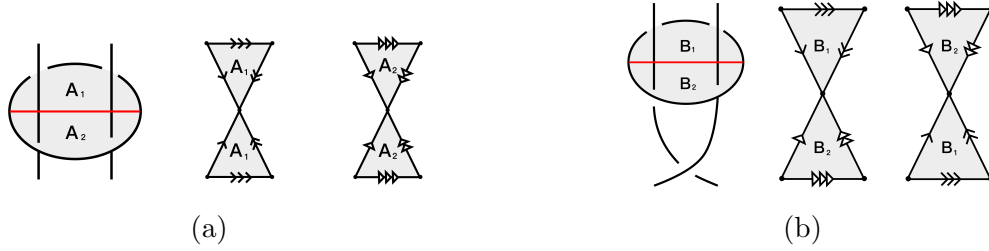


FIGURE 4. (a) Gluing of bow-ties without half-twists (b) Gluing with half-twists

the same method on the bottom half to obtain the second identical torihedron. The disk we place on each crossing circle is now cut in half. This half disk is now bounded by the projection plane and the semi-circle arc of the crossing circle. We push down on the crossing circle and split the disk into two identical disks. We then push the arc of each crossing circle to infinity, collapsing them to ideal vertices. We obtain two triangular faces which represent the disk which look like a bow-tie as in Figure 4.

We repeat the steps for the bottom half of  $\mathbb{T}^2 \times I$ ,  $\mathbb{T}^2 \times (-1, 0]$ . Then we get two torihedra. The graph of each will come from crossing edges and edges of the disk. Now, if there are half twists we will decompose the complement of the link the same way as if there are no half twists and we will identify the two bow-ties as in Figure 4. Finally, we obtain the complement of the link by gluing the two torihedra with the gluing information given by identifying crossing edges and triangles of the bow-tie. We glue the faces of the torihedra which do not correspond to a bow-tie with a  $2\pi/n$  twist where  $n$  is the number of sides of each face as in Figure 8 clockwise or counterclockwise.

For future reference, we will denote the graph for the top and bottom torihedra by  $\Gamma_T(L)$  and  $\Gamma_B(L)$ , respectively, where both graphs are viewed from the cone point of the top torihedron  $\mathbb{T}^2 \times \{1\}$ . Note that if  $L = K$  is the non-augmented link,  $\Gamma_T(L)$  is simply the link projection  $K$ , and in fact  $\Gamma_T(K) = \Gamma_B(K)$ .

□

The Figures 5 to 8 is an example which decomposes the link (C) of Figure 2.

**Definition 2.8.** An *angled torihedron*  $(\mathcal{T}, \theta_e^*)$  is a torihedron  $\mathcal{T}$  with an assignment  $\theta_e^* \in [0, \pi]$  such that for each vertex  $v \in G(\mathcal{T})$ ,  $\sum_{e \ni v} \theta_e^* = (\deg(v) - 2)\pi$ . We also denote  $\theta_e = \pi - \theta_e^*$ , so

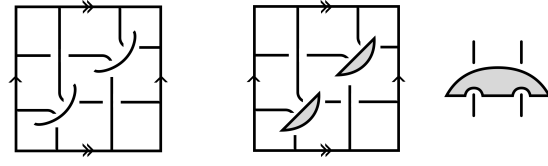


FIGURE 5. Each crossing circle bounds a twice-punctured disk

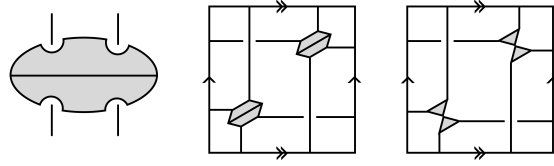


FIGURE 6. We split the disk and collapse the arc of each crossing circle to ideal vertices

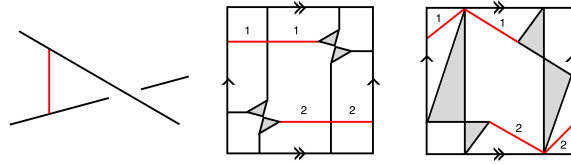


FIGURE 7. Left: The crossing arc is the edge in red. Middle: Picture of splitting the crossing edge. Right: The link component is pushed off to infinity.

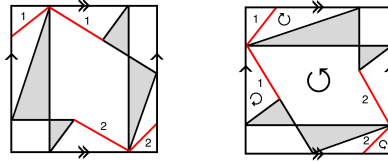


FIGURE 8. Left: The top torihedron. Right: The bottom torihedron with rotation for face gluing.

$\sum_{e \ni v} \theta_e = 2\pi$ ; we refer to  $\theta_e$  as the exterior angle and  $\theta_e^*$  as the interior angle. For brevity, we write dihedral angle to mean interior dihedral angle.

We say  $(\mathcal{T}, \theta_\bullet^*)$  is *degenerate* if  $\theta_e^* = 0$  for some edge; we say it is *non-degenerate* otherwise.

One may ask for the pyramidal decomposition of a torihedron to “respect” angles. The following definitions, in particular an “angle splitting”, make sense of this.

**Definition 2.9.** An *angled ideal tetrahedron* is an ideal tetrahedron with an assignment of a dihedral angle to each edge, such that

- each dihedral angle is in  $[0, \pi]$ ;
- for each tetrahedron, opposite edges have equal dihedral angles;
- the three distinct interior angles at edges incident to one vertex sum to  $\pi$ .

We say an angled ideal tetrahedron is *degenerate* if one dihedral angle is 0; we say it is *non-degenerate* otherwise.

**Definition 2.10.** A *base-angled ideal pyramid* is a pyramid whose base is an  $n$ -gon,  $n \geq 3$ , and each boundary edge  $e_i$  of the base face is assigned a dihedral angle  $\alpha_i \geq 0$  such that the sum is  $\sum \alpha_i = 2\pi$ . The vertical edge  $e'_i$  that meets  $e_i$  and  $e_{i+1}$  is automatically assigned the dihedral angle  $\pi - \alpha_i - \alpha_{i+1}$ .

We say a base-angled ideal pyramid is *degenerate* if  $\alpha_i = 0$  for some  $i$ ; we say it is *non-degenerate* otherwise.

Clearly, the dihedral angles of an ideal hyperbolic pyramid make it a base-angled ideal pyramid (with  $\alpha_i = \varphi_{e_i}$ ); it is not hard to see that the converse is true: simply consider a circumscribed polygon such that the side  $e_i$  subtends an angle of  $2\alpha_i$  at the center, and take the ideal hyperbolic pyramid over it in upper-half space. Also, an angled ideal tetrahedron is simply a base-angled ideal pyramid with base a triangle, and with no preferred face.

**Definition 2.11.** An *angle splitting* of an angled torihedron  $(\mathcal{T}, \theta_\bullet^*)$  is a splitting of  $\theta_e^* = \varphi_{\bar{e}} + \varphi_{\bar{e}'}^*$  for each edge  $e$ , such that for each face  $f$ ,  $\sum_{\bar{e} \in \partial f} \varphi_{\bar{e}} = \pi$ .

Equivalently, an angle splitting is a decomposition of  $\mathcal{T}$  into base-angled pyramids, one for each face of  $G(\mathcal{T})$ , such that for each boundary edge  $e$  of  $\mathcal{T}$ , the dihedral angles from the two adjacent pyramids add to  $\theta_e^*$ .

**Remark 2.12.** These  $\theta$ 's are related to the  $\theta$ 's in [3], and the  $\varphi$ 's are related to their "coherent angle system".

**Lemma 2.13.** Let  $P_n$  be a base-angled ideal pyramid, and suppose we are given a decomposition of the base face into triangles by adding new edges. One gets an obvious corresponding triangulation of  $P_n$ , where a new face is added for each new edge. Then there is an assignment of a dihedral angle to each edge of each ideal tetrahedron in this triangulation such that

- each tetrahedron is an angled ideal tetrahedron;
- the sum of dihedral angles around each new edge is  $\pi$ ;
- the dihedral angles of the edges of the original base face are the same as before.

*Proof.* Induct on  $n$ ; there is nothing to prove for the base case  $n = 3$ .

The proof is essentially given in Figure 9.

Suppose the edges are labeled  $e_i$ , for an edge which goes between vertices  $v_i$  and  $v_{i+1}$ , and suppose  $e_i$  is assigned dihedral angle  $\alpha_i$ . Let  $e'$  be a new edge added to the base face of  $P_n$  such that it separates the base face into a triangle and an  $(n-1)$ -gon; suppose the sides of the triangle are  $e_i, e_{i+1}$ , and  $e'$ . The new face corresponding to  $e'$  separates  $P_n$  into an ideal tetrahedron  $T$  and an ideal pyramid  $P_{n-1}$ . We assign the dihedral angle of  $\pi - \alpha_i - \alpha_{i+1}$  to  $e'$  in  $T$ , and assign  $\alpha_i + \alpha_{i+1}$  to  $e'$  in  $P_{n-1}$ . Clearly the sum of dihedral angles condition is satisfied in  $T$  and  $P_{n-1}$ . It remains to check that the dihedral angles assigned to the vertical (non-base) edges are correct. For the vertical edge associated to  $v_j$  for  $j \neq i, i+2$ , there is nothing to check; for  $j = i$ , the dihedral angles are  $\pi - \alpha_i - (\pi - \alpha_i - \alpha_{i-1})$  in  $T$  and  $\pi - \alpha_{i-1} - (\alpha_i + \alpha_{i+1})$  in  $P_{n-1}$ , which sum to  $\pi - \alpha_i - \alpha_{i+1}$ ; it is similar for  $j = i+2$ .

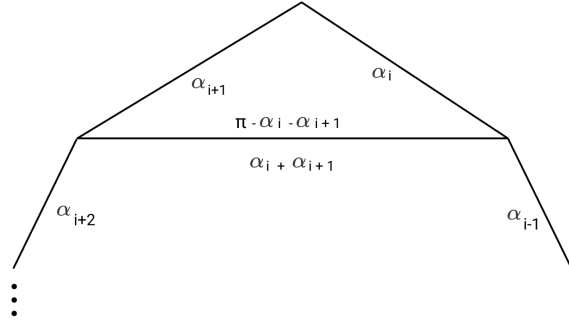


FIGURE 9. Angle-splitting on a polygonal face of the graph

□

### 3. HYPERBOLICITY OF AUGMENTED LINKS

Thurston introduced a method for finding the unique complete hyperbolic metric for a given 3-manifold  $M$  with boundary consisting of tori [10]. Thurston had written down a system of gluing and consistency equations which can be translated to equations with angles for a triangulation of  $M$  whose solutions correspond to the complete hyperbolic metric on the interior of  $M$ . Casson and Rivin separated Thurston's gluing equations into a linear and non-linear part [6]. Angle structures is the linear part of Thurston's gluing equations, and what we will use to attain hyperbolicity of complements of augmented links in the thickened torus.

**Definition 3.1.** Let  $M$  be an orientable 3-manifold with boundary consisting of tori. An angle structure on an ideal triangulation  $\tau$  of  $M$  is an assignment of a dihedral angle to each edge of each tetrahedron, such that

- each tetrahedron is a non-degenerate angled ideal tetrahedron,
- around each edge of  $\tau$ , the dihedral angles sum to  $2\pi$ .

**Theorem 3.2.** [?] *Let  $M$  be a 3-manifold admitting an angle structure. Then  $M$  is hyperbolic.*

For a hyperbolic link  $K$  in  $\mathbb{T}^2 \times I$ , we show that the resulting link obtained from augmenting  $K$  is hyperbolic. The idea is to start with a graph from the torihedral decomposition of the link  $K$  which will give us a graph on each torihedron with an angle assignment of  $\pi/2$  for edge [4]. By Proposition 2.7, there is a torihedral decomposition of the complement of the augmented link  $L$ . Using those angles from  $K$ , we then assign new angles locally to edges of torihedra from a torihedral decomposition of  $L$  and decompose them into base-angled pyramids which can be decomposed into tetrahedra, thus obtaining an angle structure on a triangulation.

**Definition 3.3.** We say an augmentation is *right-augmented* if, when both strands are (locally) oriented so that they cross the augmentation disk in the same direction, the crossing between them is a positive right-handed half-twist. See Figure 10. We say an augmentation is *left-augmented* if it is not right-augmented.

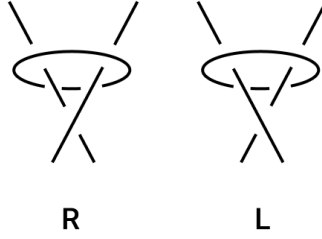


FIGURE 10. R: right augmentation, L: left augmentation

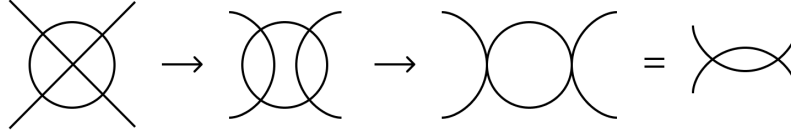


FIGURE 11. Resolving internal vertex; eliminating bigons via “crushing”

We can recover  $L$  from the link diagram of  $K$  together with labels at vertices indicating left- or right-augmentation.

**Lemma 3.4.** *Let  $G$  be a 4-valent graph on  $\mathbb{T}^2$  with no bigons or self-loops. Then for any subset  $F' \subseteq F$  of faces,*

$$2\chi(F') \leq |E'|$$

*where  $E' = \cup_{f \in F'} \partial f$  is the set of edges that meets some face of  $F'$ , and  $\chi(F') = \sum_{f \in F'} \chi(f)$  is the sum of the Euler characteristics of faces in  $F'$ .*

*Proof.* We induct on  $\chi(F')$  (over all possible such graphs  $G$ ); for  $F' = \emptyset$  or  $\chi(F') \leq 0$ , there is nothing to prove.

Call a vertex or edge *interior* if it does not meet  $F'' = F \setminus F'$ . Suppose there is an interior vertex  $v$ . Make the modification as in Figure 11 (later we will choose which way to “resolve” the vertex). This decreases  $\chi(F')$  by one and  $|E'|$  by 2. However, this process may produce bigons; if it does, repeatedly eliminate bigons by either (1) performing the modification as in Figure 11 if the two vertices of the bigon are distinct, or (2) remove the bigon completely if the two vertices of the bigon are the same. Each of these steps also decreases  $\chi(F')$  by one and  $|E'|$  by 2 (note in the second case, after removing the bigon, the operation merges two distinct faces or joins a face to itself; this adds an  $S^1$ , thus does not change the (total) euler characteristic of the two faces or the one face).

We must check that this process terminates with a graph which satisfies the hypotheses set out in the lemma. It is clear that 4-valency is maintained at each step, and there will not be any bigons at the end. We need to ensure that eliminating bigons does not create self-loop edges. Here we specify how to choose which way to resolve the internal vertex  $v$ . If among the four faces touching  $v$ , one of them has greater than three sides (Case 1), then resolve  $v$  so that this face is not merged; if all four faces are triangles (Case 2), simply resolve in an arbitrary manner. After the modification of the internal vertex, at most two bigons are created; eliminate those two bigons. Now we find that all bigons will be connected end-to-end (i.e. forming a single twist region) - this is because in Case 1, only one bigon was present



after smoothing  $v$ , which would result in at most two bigons that would be connected; and if we were in Case 2, we find that the face between those eliminated bigons (coming from merging the two triangles across  $v$ ) will become a bigon too, thus connecting the potential bigons on either ends.

Therefore, one can eliminate bigons in an order so that they belong in one twist region; in particular, the (not necessarily distinct) faces on either side are not bigons, so eliminating the bigon does not produce a self-loop edge.

Now suppose  $G$  has no interior vertices. We perform some reductions. We remove all  $f$  from  $F'$  that have non-positive Euler characteristic, as doing so will not decrease  $\chi(F')$  and will not increase  $|E'|$ . Now consider some  $f \in F'$ . If it has at least two boundary (i.e. non-interior) edges, we can remove  $f$  from  $F'$ , which decreases  $\chi(F')$  by 1 and  $|E'|$  by at least 2. Thus we remove all such  $f$ .

Now suppose  $f \in F'$  has three contiguous interior edges  $e_1, e_2, e_3$ . (e.g. if  $f$  has at least four sides). Let  $v_1, v_2$  be the vertices between these three interior edges. Since  $v_1$  is not interior, the face across  $v_1$  from  $f$  is not in  $F'$ ; likewise with  $v_2$ . But this shows that the face across  $e_2$  from  $f$  has two boundary edges, contradicting our reduction.

Thus, we now have a graph whose faces are triangles, and each face has exactly one boundary edge. Now the problem is solved with a simple counting argument: each  $f$  corresponds to one boundary edge and two interior edges, but, since the interior edges are shared by two faces, they should count as half an edge; so

$$|E'| = \sum_{f \in F'} 1 + 1/2 + 1/2 = 2|F'| = 2\chi(F')$$

and we get the desired result.  $\square$

The following theorem is quoted from [3] (see also [5])

**Theorem 3.5** (Feasible Flow Theorem). *Let  $(N, X)$  be a directed graph, with a lower capacity bound  $a_x$  and upper capacity bound  $b_x$  for each directed edge  $x \in X$ , with  $-\infty \leq a_x \leq b_x \leq \infty$ . A feasible flow is a function  $\varphi : X \rightarrow \mathbb{R}$  such that  $\varphi_x \in [a_x, b_x]$  and Kirchhof's current law is satisfied (i.e. flow in = flow out at every vertex).*

*A feasible flow exists if and only if, for every proper nonempty subset  $N' \subset N$ ,*

$$\sum_{x \in \text{ex}(N')} b_x \geq \sum_{x \in \text{in}(N')} a_x$$

*where  $\text{ex}(N'), \text{in}(N')$  refer to edges leaving, entering  $N'$ , respectively.*

**Theorem 3.6.** *Let  $K$  be a weakly prime, alternating link whose diagram has no bigons. Let  $L$  be a link obtained from augmenting  $K$ . Then  $L$  is hyperbolic.*

*Proof.* By [4, Theorem 7.5], (as discussed in Proposition 2.7,)  $\mathbb{T}^2 \times I - K$  can be decomposed into two torihedra  $\mathcal{T}_T$  and  $\mathcal{T}_B$ , whose graphs are  $\Gamma_T(K), \Gamma_B(K)$  respectively; viewed from the top cone point  $\mathbb{T}^2 \times \{1\}$ , they are both the same as the projection graph of  $K$ . We make them non-degenerate angled torihedra by assigning  $\theta^* = \pi/2$  for all edges. Unlike in the case of alternating links or fully augmented links in the thickened torus we cannot make all angles  $\pi/2$ . This is because in our decomposition the vertices of the graph which defines our torihedra are not all four valent.

We obtain an angle-splitting by applying the Feasible Flow theorem (Theorem 3.5) as follows: Consider the directed graph whose vertex set is  $E \cup F \cup \{*\}$ , where  $E, F$  are the set of edges, faces of  $\Gamma_T(K)$  respectively, and there is a directed edge

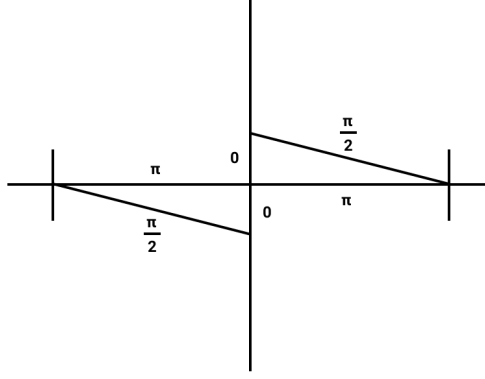


FIGURE 12. Angle assignments on a bow-tie corresponding to an augmentation site

- $* \rightarrow f$  for each face  $f \in F$ , with capacity interval  $[\pi, \infty)$ ,
- $f \rightarrow e$  for each edge  $e \in \partial f$ , with capacity interval  $[\varepsilon, \infty)$  for some  $\varepsilon > 0$  to be set later,
- $e \rightarrow *$  for each edge  $e$ , with capacity interval  $(-\infty, \pi/2]$ .

By Lemma 3.4,  $2|F'| = 2\chi(F') \leq |E'|$ , and taking  $\varepsilon < \pi/|\max \text{ face size}|$ , the feasible flow condition is satisfied, so a feasible flow exists. Since  $2|F| = |E|$ , the capacity interval restrictions on the flow at  $*$  is sharp, so out-edges at  $*$  have flow  $\pi$  and in-edges at  $*$  have flow  $\pi/2$ . Then the flow  $f \rightarrow e$  gives us  $\varphi_{\vec{e}}$ , where  $f$  is the face to the left of  $\vec{e}$ . (We adapted this argument from Lemma 3.4 of [3]).

By Proposition 2.7,  $\mathbb{T}^2 \times I - L$  can be obtained by gluing two torihedra  $\mathcal{T}_T(L), \mathcal{T}_B(L)$  with graphs  $\Gamma_T(L), \Gamma_B(L)$ . We make them degenerate angled torihedra by assigning  $\theta^*$ 's to edges of the bow-ties as in Figure 12, and assign  $\pi/2$  to all other edges. It is easy to check that upon gluing, each edge has sum of dihedral angles ( $\theta^*$ ) that is equal to  $2\pi$ . (This holds true even if they were glued assuming some augmentations had no half-twist; see Remark 3.7.)

Furthermore, we can obtain an angle-splitting of  $\mathcal{T}_T(L)$  (and similarly  $\mathcal{T}_B(L)$ ) by modifying the angle-splitting for  $\mathcal{T}_T(K)$ ; this is shown in Figure 13.

Now we have a decomposition of the two torihedra into degenerate base-angled pyramids. However, we need the pyramids to be non-degenerate, so we first need to modify the angles and graph on the torihedra to make all  $\theta^*$  nonzero.

Consider a face  $f$  of  $\Gamma_T(L)$  that is not in a bow-tie. Suppose the corresponding face  $\bar{f}$  of  $\Gamma$ , the projection graph (which is equal to  $\Gamma_T(K)$ ), had vertices  $v_1, \dots, v_n$  in counter-clockwise order. We label the edges of  $f$  by  $e_{i,0}$ ,  $e_{i,\pi}$ , or  $e_i$ , depending on whether the  $\theta^*$  is 0,  $\pi$ , or  $\pi/2$  respectively, with  $i$  non-decreasing from 1 to  $n$ , adjacent edges having the same  $i$  if and only if they belong to the same bow-tie. For sake of concreteness, suppose that if a vertex  $v_i$  is right-augmented, then the augmentation circle intersects  $\bar{f}$  (everything is similar if it is left-augmented vertices' circles that intersect  $\bar{f}$ ). In other words, locally,  $f$  meets two of the edges of the bow-tie corresponding to a right-augmented vertex  $v_i$  (which would be labeled  $e_{i,0}, e_{i,\pi}$  in counter-clockwise order), but only meets one of the edges of the bow-tie corresponding to a left-augmented vertex.

Suppose, after cyclically reindexing,  $v_1, \dots, v_k$  is a maximally contiguous subsequence of left-augmented vertices of  $G(K)$  around the face  $\bar{f}$ ; the edges around  $f$  would start

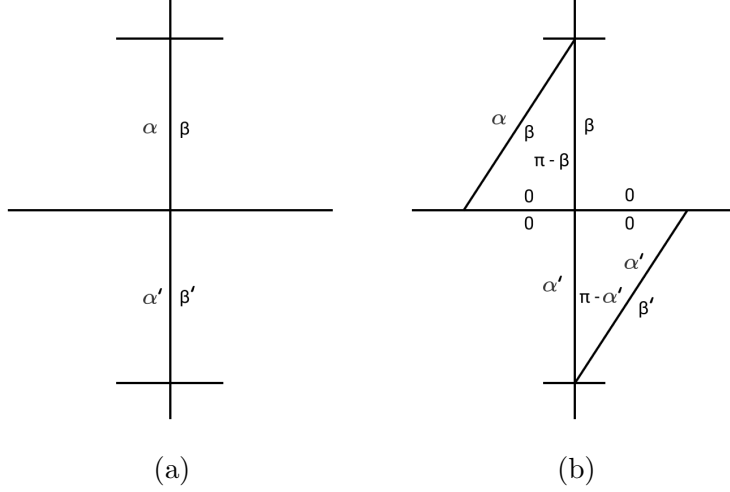


FIGURE 13. (a) Angles before augmentation (b) Angle splitting for bowtie corresponding to augmentation

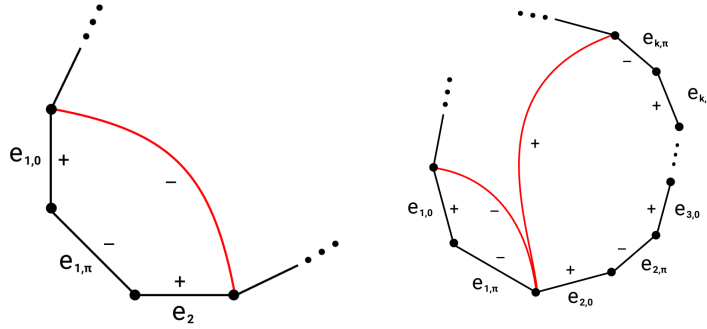


FIGURE 14. Red edge indicates an added edge to the graph to appropriately assign +/- labels which indicate increasing/decreasing angles on the edge respectively.

$e_{1,0}, e_{1,\pi}, e_{2,0}, e_{2,\pi}, \dots$ . We add new edges across  $f$  as follows. (See Figure 14; ignore the + and - signs for now.)

First suppose  $k = n$ ; then we do nothing.

Next suppose there is only one such maximal contiguous subsequence. If  $k = 1$ , we add an edge that goes across  $e_{1,0}, e_{1,\pi}, e_2$  (in the sense that the new edge separates the edges of  $f$  into two sets, one of them being those three edges; since  $n \geq 3$ , this edge is new). If  $k \geq 2$ , we add an edge across  $e_{1,0}, e_{1,\pi}$  and another edge across  $e_{2,0}, e_{2,\pi}, e_{3,0}, \dots, e_{k,\pi}$  (these two edges do not form a bigon because we've ruled out  $k = n$ ).

Finally, if there are multiple such maximal contiguous subsequences, we just add edges as above for each contiguous subsequence. The only caveat is that if the procedure calls to add a new edge that would form a bigon with the existing edges, we just do not add it.

This way we obtain a new graph  $\Gamma_T(L)'$ , which defines a new torihedron  $\mathcal{T}_T(L)'$ . We make  $\mathcal{T}_T(L)'$  angled using the angles from  $\mathcal{T}_T(L)$  for old edges, and putting  $\pi$  for all new edges.

Now we deform the  $\theta^*$  based on Figure 14, increasing/decreasing by some small  $\varepsilon' > 0$  if the edge is labeled  $+/-$ . Note some edges may be labeled twice, in which case we perform both increasing/decreasing (e.g. if it is labeled  $+$  and  $-$ , the  $\theta^*$  is not changed). It is easy to see that the sum of  $\theta^*$  around a vertex remains unchanged. Furthermore, all the edges with  $\theta^*$  originally equal 0, i.e. all  $e_{i,0}$ 's, now have positive  $\theta^*$ , (it receives only one label  $+$ , because the other face it meets is a bow-tie).

We can directly get an angle-splitting for  $\mathcal{T}_T(L)'$  using the angle-splitting for  $\mathcal{T}_T(L)$ . We reuse the  $+/-$  assignments from Figure 14. For  $e = e_{i,0}$ , we increase  $\varphi_{\vec{e}}, \varphi_{\leftarrow e}$  by  $\varepsilon'/2$  each; for  $e = e_{i,\pi}$ , we decrease them by  $\varepsilon'/2$  each. For other edges, we increase/decrease  $\varphi_{\vec{e}}$  by  $\varepsilon'$ , where  $\vec{e}$  is the oriented edge corresponding to the side on which the  $+/-$  sign appears in Figure 14; so for example, if an edge  $e$  receives both  $+$  and  $-$ , then one of  $\varphi_{\vec{e}}, \varphi_{\leftarrow e}$  increases while the other decreases, thus  $\theta_e^*$  remains constant.

Now we address  $\mathcal{T}_B(L)$ . In the gluing of  $\mathcal{T}_T(L)$  to  $\mathcal{T}_B(L)$ , non-bow-tie faces of  $\Gamma_T(L)$  are identified with non-bow-tie faces of  $\Gamma_B(L)$ . Under this identification, we add the same edges to  $\Gamma_B(L)$ , thus obtaining the new torihedron  $\mathcal{T}_B(L)'$  with graph  $\Gamma_B(L)'$ . We perform the same deformations of  $\theta^*$ 's (or  $\varphi$ 's).

We need to check that upon gluing  $\mathcal{T}_T(L)'$  to  $\mathcal{T}_B(L)'$ , the sum of dihedral angles around each edge is still  $2\pi$ . This was clearly true before deforming, as the new edges of  $\Gamma_T(L)'$  only gets identified with the unique corresponding edge of  $\Gamma_B(L)'$ , and they are both labeled with  $\theta^* = \pi$ . To see that the deformation does not change these sums, note that in the identification of faces of  $\Gamma_T(L)'$  to  $\Gamma_B(L)'$ , an edge with  $\theta^* = 0$  is identified with an edge with  $\theta^* = \pi$ , so an increase in the former would be counterbalanced by a decrease in the latter. It is also easy to see this is the case for the other edges. (Once again, a similar argument applies if  $\mathcal{T}_T(L)'$  and  $\mathcal{T}_B(L)'$  are glued assuming some augmentations had no half-twist; see Remark 3.7.)

Finally, for each face of  $\Gamma_T(L)'$  that has more than three sides, we arbitrarily decompose it into triangles and apply Lemma 2.13 to obtain a triangulation of  $\mathcal{T}_T(L)'$  into non-degenerate angled tetrahedra; perform the corresponding decomposition for faces of  $\Gamma_B(L)'$  and obtain a triangulation of  $\mathcal{T}_B(L)'$  into non-degenerate angled tetrahedra. Upon gluing, this gives an angle structure on the triangulation of  $\mathbb{T}^2 \times I - L$   $\square$

**Remark 3.7.** If the original link  $K$  had some twist regions with at least one bigon, we may consider augmentations  $L$  where all such twist regions are augmented, i.e.  $L$  may have augmentations without half-twists. Then, as pointed out in proof of Theorem 3.6 above, the proof still works for  $L$ , showing that  $L$  is also hyperbolic.

## REFERENCES

- [1] Colin Adams, Michele Capovilla-Searle, Darin Li, Qiao Li, Jacob McErlean, Alexander Simons, Natalie Stewart, and Xiwen Wang. Generalized augmented cellular alternating links in thickened surfaces are hyperbolic. *arXiv preprint arXiv:2107.05406*, 2021.
- [2] Colin C. Adams. Augmented alternating link complements are hyperbolic. In *Low-dimensional topology and Kleinian groups (Coventry/Durham, 1984)*, volume 112 of *London Math. Soc. Lecture Note Ser.*, pages 115–130. Cambridge Univ. Press, Cambridge, 1986.
- [3] Alexander I. Bobenko and Boris A. Springborn. Variational principles for circle patterns and Koebe's theorem. *Trans. Amer. Math. Soc.*, 356(2):659–689, 2004.
- [4] Abhijit Champanerkar, Ilya Kofman, and Jessica S. Purcell. Geometry of bi-periodic alternating links. *J. Lond. Math. Soc. (2)*, 99(3):807–830, 2019.
- [5] L. R. Ford, Jr. and D. R. Fulkerson. *Flows in networks*. Princeton Landmarks in Mathematics. Princeton University Press, Princeton, NJ, 2010. Paperback edition [of MR0159700], With a new foreword by Robert G. Bland and James B. Orlin.

- [6] David Futer and François Guéritaud. From angled triangulations to hyperbolic structures. In *Interactions between hyperbolic geometry, quantum topology and number theory*, volume 541 of *Contemp. Math.*, pages 159–182. Amer. Math. Soc., Providence, RI, 2011.
- [7] Alice Kwon. Fully augmented links in the thickened torus. *arXiv preprint arXiv:2007.12773*, 2020.
- [8] Marc Lackenby. The volume of hyperbolic alternating link complements. *Proc. London Math. Soc. (3)*, 88(1):204–224, 2004. With an appendix by Ian Agol and Dylan Thurston.
- [9] William W. Menasco. Polyhedra representation of link complements. In *Low-dimensional topology (San Francisco, Calif., 1981)*, volume 20 of *Contemp. Math.*, pages 305–325. Amer. Math. Soc., Providence, RI, 1983.
- [10] W. P. Thurston. The geometry and topology of three-manifolds. Princeton Univ. Math. Dept. Notes. Available at <http://www.msri.org/communications/books/gt3m>. [2, 21, 50, 58, 68, 87, 89, 94, 97, 99, 138, 196], 1979.